Remote Sensing of Environment 123 (2012) 81–89

Contents lists available at SciVerse ScienceDirect

Remote Sensing of Environment

journal homepage: www.elsevier.com/locate/rse

Characterization of canopy fuels using ICESat/GLAS data

Mariano García [a,*], Sorin Popescu [b], David Riaño [c,d], Kaiguang Zhao [e], Amy Neuenschwander [f], Muge Agca [g], Emilio Chuvieco [a]

[a] COMPLUTIG-UAH, Department of Geography, University of Alcalá, C/ Colegios, 2, Alcalá de Henares, 28801, Madrid, Spain
[b] Spatial Sciences Laboratory, Department of Ecosystem Science and Management, Texas A&M University, 1500 Research Parkway, Suite B 223, TAMU 2120, College Station, TX 77845, United States
[c] Institute of Economics and Geography, Spanish National Research Council (CSIC), Albasanz 26-28 28037 Madrid, Spain
[d] Center for Spatial Technologies and Remote Sensing (CSTARS), University of California, 250-N, The Barn, One Shields Avenue, Davis, CA 95616-8617, United States
[e] Center on Global Change, Nicholas School of the Environment, Duke University, Durham, NC 27708, United States
[f] Applied Research Laboratories, University of Texas at Austin, Austin, TX 78758, United States
[g] Aksaray University, Faculty of Engineering, Department of Geomatics Engineering, 68100 Aksary, Turkey

ARTICLE INFO

Article history:
Received 8 February 2011
Received in revised form 24 February 2012
Accepted 16 March 2012
Available online xxxx

Keywords:
ICESat/GLAS
Canopy fuels
Canopy cover
LAI
Canopy bulk density

ABSTRACT

This study aimed to estimate canopy fuel properties relevant for crown fire behavior using ICESat/GLAS satellite LiDAR data. GLAS estimates were compared to canopy fuel products generated from airborne LiDAR data, which had been previously validated against field data. The geolocation accuracy of the data was evaluated by comparing ground elevation on both datasets, showing an offset of 1 pixel (20 m). Canopy cover (CC) was estimated as the ratio of the canopy energy to the total energy of the waveform. Application of a canopy base height threshold (CBH) to compute the canopy energy increased the accuracy of CC estimates ($R^2 = 0.89$; RMSE = 16.12%) and yielded a linear relationship with airborne LiDAR estimates. In addition, better agreement was obtained when the CC derived from airborne LiDAR data was estimated using the intensity of the returns. An empirical model, based on the CC and the leading edge (LE), was derived to estimate leaf area index (LAI) using stepwise regression providing good agreement with the reference data ($R^2 = 0.9$, RMSE = 0.15). Canopy bulk density (CBD) was estimated using an approach based on the method developed by Sando and Wick (1972) to derive CBD from field measurements, and adapted to GLAS data. Thus, foliage biomass was distributed vertically throughout the canopy extent based on the distribution of canopy material and CBD was estimated as the maximum 3 m-deep running mean considering layers with a thickness of 15 cm, which is the vertical resolution of the GLAS data. This approach gave a coefficient of determination of 0.78 and an RMSE of 0.02 kg m^{-3}.

1. Introduction

In order to perform appropriate fire planning and management activities such as predicting fire behavior and effects, or designing fuel treatment to reduce potential damage caused by fires, accurate spatial fuel properties information is required (Reeves et al., 2009; Sandberg et al., 2001). This need becomes especially important when dealing with crown fires because they are more difficult to control than surface fires. Once crowning occurs, there is an increase in the rate of spread, intensity and spotting. Moreover, the effects of crown fires are more severe and lasting than surface fires (Scott & Reinhardt, 2001). Knowledge of fuel properties is not only important to fire managers but also to ecologists, air quality managers and carbon balance modelers (Sandberg et al., 2001).

Airborne light detection and ranging (LiDAR) is an active remote sensing technology that has been proven to be suitable to estimate canopy properties relevant for crown fire behavior and effects, such as canopy base height (CBH), canopy fuel load (CFL), canopy cover (CC) or canopy bulk density (CBD). CBH, which represents the distance from the ground to the minimum amount of fuel required to allow vertical propagation of fire through the canopy (Scott & Reinhardt, 2001), has been successfully estimated via regression analysis (Andersen et al., 2005; Erdody & Moskal, 2009; Hall et al., 2005), by finding the inflection point after the maximum of a fourth-degree polynomial fitted to the canopy vertical profile (Popescu & Zhao, 2008), or by clustering analysis (Morsdorf et al., 2004; Riaño et al., 2003). CFL, expressed as dry biomass per unit area, represents the amount of fuel that is potentially available for combustion (Chuvieco et al., 2003) and has been estimated using LiDAR data by means of regression analysis (Erdody & Moskal, 2009; Hall et al., 2005).

CBD can be defined as the mass of available canopy fuel per unit canopy volume that would burn in a crown fire (Scott & Reinhardt, 2001). Some differences can be found in the literature to define the

* Corresponding author.
E-mail addresses: mariano.garcia@uah.es (M. García), david.riano@cchs.csic.es (D. Riaño).

0034-4257/$ – see front matter © 2012 Elsevier Inc. All rights reserved.
doi:10.1016/j.rse.2012.03.018

available fuel. Thus, whereas some researchers consider only the foliage biomass (Keane et al., 2005; Riaño et al., 2003; Van Wagner, 1977), others include foliage, lichen, moss and a portion of small branches that would be consumed in the flaming front (Keane et al., 2005; Scott & Reinhardt, 2001). LiDAR data have been proven to be suitable to estimate CBD by means of regression analysis (Andersen et al., 2005; Erdody & Moskal, 2009; Hall et al., 2005). A different approach was employed by Riaño et al. (2003) and Riaño et al. (2004a) who estimated crown bulk density, a property of individual trees rather than a stand property, by dividing the foliage biomass by the crown volume, both previously derived from LiDAR data. CC, which is defined as the vertical projection of crowns on the ground, provides a representation of the horizontal distribution of fuels. In addition, CC indirectly influences crown fire behavior through its effects on fine fuel moisture content and the wind reduction factor (Albini & Baughman, 1979; Rothermel et al., 1986). CC has been derived from discrete return LiDAR either as a function of the proportion of canopy returns (Morsdorf et al., 2006; Riaño et al., 2004b) or as the proportion of the intensity of canopy returns (García et al., 2010; Solberg et al., 2009).

Another important variable for crown fire is the leaf area index (LAI), which is defined as the ratio of the one-sided surface area of leaves to the projected ground area ($m^2\,m^{-2}$) (Lefsky et al., 1999). LAI can be used to compute foliage biomass by using the specific leaf area (SLA) and so, it can be employed to derive canopy fuel load and canopy bulk density. LiDAR data have been successfully employed to estimate LAI in different environments (Morsdorf et al., 2006; Riaño et al., 2004b; Solberg et al., 2009).

Full waveform systems, which are able to record the whole backscattered signal, have also been successfully used to estimate canopy properties as demonstrated by several studies (Lefsky et al., 1999; Means et al., 1999; Peterson, 2005).

Despite the potential shown by airborne LiDAR to estimate important canopy fuel properties, its use is limited to local or regional scales (Zhao & Popescu, 2009). This limitation in terms of spatial coverage can be overcome by the Geoscience Laser Altimeter System (GLAS) onboard of the Ice Cloud and land Elevation Satellite (ICESat), which is the first LiDAR system designed to provide a continuous coverage of the Earth (Zwally et al., 2002).

The ICESat/GLAS satellite was launched on 13 January, 2003 and was primarily designed to determine changes in polar ice-sheet mass and its causes and effects. Additionally it also provides observations of land topography and vegetation as well as global measurements of clouds and aerosols (Zwally et al., 2002). ICESat was launched into a 600 km altitude orbit with a 94° inclination and included the GLAS sensor onboard, which carried three lasers. The GLAS sensor emitted laser pulses at 1064 nm and 532 nm for surface and atmospheric observations, respectively; with an outgoing pulse width of 7–8 ns and at a laser repetition rate of 40 Hz. The sensor recorded the returned energy from an elliptical footprint (assuming a $1/e^2$ energy distribution) with a nominal diameter of about 70 m, although its size and ellipticity have changed through time (Carabajal & Harding, 2006). Data were collected in the form of transects of individual waveform observations, which were spaced approximately 175 m along track and a maximum of 15 km across track at the equator (Zwally et al., 2002). Originally, the ICESat mission was conceived to provide continuous observation of the Earth throughout its lifetime, but due to the rapid degradation of the lasers the mission was reconfigured to 33-day operational campaigns, three times per year, to meet mission requirements (Schutz et al., 2005). Each campaign is identified by the laser number (1–3) and a letter (A–K) to designate the operational period. The last campaign was carried out in October 2009.

In the last few years a number of investigations have shown the capability of GLAS data to estimate vegetation parameters. Vegetation height has been estimated either directly from the waveform (Neuenschwander et al., 2008; Sun et al., 2008) or using empirical methods (Chen, 2010; Lefsky et al., 2007; Xing et al., 2010). Over areas with large changes in relief and complex terrain, where the energy from ground and low vegetation can be mixed, the identification of ground elevation is more difficult, hampering the estimation of the vegetation height. Thus, methods have been proposed to improve height estimation using ancillary data by means of linear functions (Lefsky et al., 2006), non linear models (Xing et al., 2010) or models derived using the information from the waveforms themselves (Chen, 2010; Lefsky et al., 2007). Lefsky (2010) generated a global canopy height map by integrating GLAS data and 32-day composites derived from the MODIS-MOD09A1 product. Thus, the height estimated from GLAS data was assigned to those patches that included LiDAR waveforms, whereas for patches that did not include GLAS data, canopy height was estimated using statistical modeling. Boudreau et al. (2008) provided regional estimates of aboveground biomass in Québec, Canada, by applying a scaling-up approach. First, allometric equations were developed, relating field measurements to airborne LiDAR data. Subsequently, LiDAR estimates were used to develop an empirical model to estimate biomass from GLAS data. Nelson (2010) evaluated four models in the same region to conduct regional aboveground biomass and carbon inventories using a satellite LiDAR. Popescu et al. (2011) also found good correlation between GLAS estimates of aboveground biomass and airborne LiDAR estimates over an area in Texas. Ashworth et al. (2010) evaluated the capability of GLAS data to estimate vegetation height and to identify two representative fuel models in East-Central Mississippi using logistic regression.

As has been described above, a common approach to estimate fuel properties from LiDAR data is to develop empirical models based on regression analysis. Although these models can provide accurate estimations of fuel properties, their application to different regions is limited to areas presenting the same species and environmental characteristics, constraining their applicability to regional or global scales.

The aim of this research was to evaluate the potential of GLAS data to estimate important canopy fuel properties for crown fire behavior as compared to estimates derived from airborne LiDAR data. The specific objectives were: 1) to estimate CC and analyze the effect of using different CBH thresholds, 2) to estimate leaf area index, and 3) to derive canopy bulk density. In addition, an effort is done to estimate these properties from data derived solely from the waveforms themselves in order to provide methods that could be applied at global scales to fully exploit the global coverage provided by the GLAS sensor. Similar to Popescu et al. (2011) and Neuenschwander et al. (2008), this study employs the actual elliptical shape by taking into account the major and minor axes information derived from the Laser Profile Array (LPA) (Neuenschwander et al., 2008).

2. Methods

2.1. Study area

The study area covers approximately 4800 ha and is located in the eastern half of Texas (30° 42′ N, 95° 23′ W) (Fig. 1). It mainly comprises pine plantations in various developmental stages; old growth pine stands in the Sam Houston National Forest many of which have a natural pine stand structure; and upland and bottomland hardwoods. The major species include Loblolly pines (*Pinus taeda* L.) as well as deciduous trees such as water oak (*Quercus nigra* L.), red oak (*Quercus falcata* Michx), sweetgum (*Liquidambar styraciflua* L.), and post oak (*Quercus stellata* Wangenh.). The area is also characterized by gentle slopes and an average elevation of 85 m, ranging from 62 m to 105 m.

2.2. Airborne LiDAR data

Airborne LiDAR data were acquired in March 2004 using a Leica-Geosystems ALS40 during the leaf-off season, with a mean flight

Fig. 1. Quickbird image of the study area. ICESat-GLAS footprints are overlapped to the image (black ellipses).

altitude of 1000 m. For each pulse, the X, Y, Z triplets of coordinates of first and last returns, together with their intensity were recorded. The reported accuracies of these data were 30 cm and 15 cm in the horizontal and vertical planes respectively. The maximum scan angle was set to $\pm 10°$ from nadir, yielding a swath of 350 m on the ground. The site was flown in north–south direction (19 flight lines) and in the east–west direction (28 flight lines) resulting in an average point density of 2.6 hits/m^2. The data vendor also provided a digital elevation model (DEM) with a spatial resolution of 2.5 m, generated using a proprietary ground-filtering package.

2.3. ICESat-GLAS data

GLAS data are distributed in 15 different products. For this study the GLA01 (L1A Global Altimetry Data) and GLA14 (L2 Global Land Surface Altimetry Data) products of release 28 were requested from http://www.nsidc.org/data/icesat/order.html via the GLAS data subsetter.

In order to keep the time gap between airborne and satellite LiDAR data to a minimum the GLAS products obtained on Day 51 (February) of 2004, corresponding to the observation campaign L2B, were used. It is important to use data captured on dates close together to avoid differences caused by seasonal effects on vegetation, which would introduce variability and inconsistency into the results.

The GLA01 product provides the waveform for each laser pulse. The returned energy is digitized in 544 bins recorded at 1 ns rate, which equates to 15 cm based on the speed of light. From acquisition campaign L3A, the first 151 bins were changed to 60 cm (4 ns), which resulted in an increased in the waveform length from 81.6 m to nearly 150 m. GLA01 also includes an estimated geolocation for all 40 pulses acquired within 1 s. The GLA14 product does not contain the waveform but a set of parameters derived from the waveform data in combination with precise position data obtained by the precise orbit determination (POD) and precise altitude determination (PAD) system (Duong et al., 2009). As part of the standard ICESat processing, the waveforms are smoothed by applying Gaussian filters and a noise threshold to identify the signal beginning and end, that is, the first and last height bins where the returned energy is detected above the noise threshold. Since the transmitted pulse is expected to be Gaussian, the waveform can be mathematically represented as a sum of Gaussians plus a bias (Brenner et al., 2003; Hofton et al., 2000). Initially, many Gaussian peaks are fitted to the waveform at different heights, which are subsequently reduced to a maximum of six, based on the area of each Gaussian, through an iterative process (Brenner et al., 2003; Harding & Carabajal, 2005). The GLA14 product provides the surface elevation, which corresponds to the centroid of the received waveform between signal start and end (Harding & Carabajal, 2005); and the laser range offsets for the signal beginning and end, as well as location, amplitude and width, computed using non linear least squares (Brenner et al., 2003), of the Gaussian peaks fitted to the waveform (Fig. 2).

2.4. Airborne LiDAR data processing

Airborne LiDAR data described in Section 2.2 were used to generate a set of canopy fuel property layers, which were subsequently used as reference data with which to compare GLAS estimates, that is, were used as *ground truth*. Zhao and Popescu (2009) evaluated the capability of airborne LiDAR data to estimate LAI over the same area used in this study. Based on an empirical model, they created an LAI image of the study area with a spatial resolution of 20 m, which was found as an appropriate scale for applying the LAI model they had obtained. This model was able to explain 84% of the variation of field-measured LAI with an RMSE of 0.29.

The CC reference-images used to validate the CC estimated using GLAS data were generated as the proportion of canopy returns to all returns within each pixel. A 20 m spatial resolution was used to match that of the LAI image derived by Zhao and Popescu (2009). CC images were also obtained by using the intensity of returns after normalization of intensity values by removing the range dependency of the data (Donoghue et al., 2007; García et al., 2010; Starek et al., 2006). Canopy returns were considered as vegetation returns with a height greater than or equal to 2 m.

The CBD reference data used in this study was created by Zhao et al. (2011), who developed a model based on machine learning

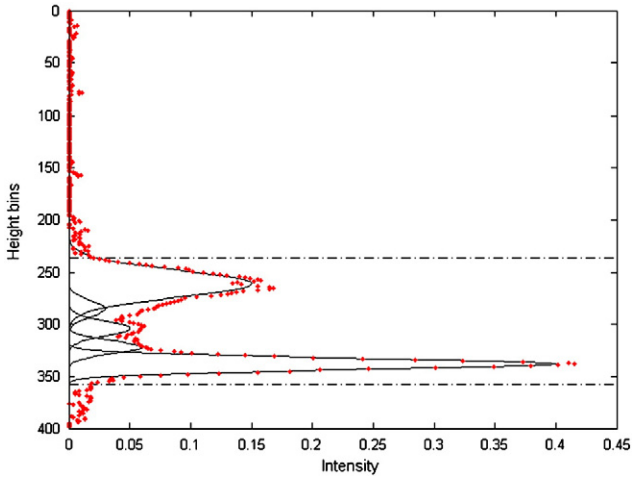

Fig. 2. Example of a received waveform (red dots), the signal beginning and end (black dash-dotted line) and the Gaussians fitted to the waveform (black solid line). (For interpretation of the references to color in this figure legend, the reader is referred to the web version of this article.)

techniques to relate field based estimates of CBD to airborne LiDAR metrics. The selected model was validated using field measurements and yielded an R^2 of 0.76 and an RMSE of 0.015 kg m^{-3}. No image was generated for CBD but the reference data were generated for each footprint.

2.5. GLAS data processing

Both products, GLA01 and GLA14, were merged based on the record index and the shot number, and were subsequently processed to extract a set of metrics. Saturated waveforms that could occur due to the automatic gain adjustment of the sensor were excluded from the analysis leaving 32 footprints available for analysis over the study area. For each footprint the following metrics were derived from the waveform data. First, considering the total waveform energy, the 25th, 50th (height of median energy-HOME), 75th and 90th percentiles of the energy were derived relative to the ground elevation (last Gaussian peak), as well as the skewness of the waveform. These variables have been shown to be useful to estimate structural attributes (Drake et al., 2002; Sun et al., 2008).

The height/median ratio (HTRT), which provides an index of how the location of HOME may change relative to canopy height, was derived by dividing HOME by the canopy height (Drake et al., 2002). Canopy height (CH) was estimated as the height of the signal beginning. By calculating the slope between the signal beginning and the first Gaussian canopy peak, the front slope angle (FSA) was computed. This variable provides information on canopy density and the vertical variability of the upper canopy (Boudreau et al., 2008). Following Lefsky et al. (2007) the leading edge (LE), which is related to the canopy height variability, as well as the trailing edge (TE), related to the slope, were computed for each waveform.

Lefsky et al. (1999) proposed a modification of the MacArthur and Horn's (1969) method to describe the canopy structure based on the canopy height profile (CHP). Two measurements of the average height of the CHP were calculated, namely the mean canopy height (MCH) and the quadratic mean canopy height (QMCH). The rise time to the first peak (Neuenschwander et al., 2009), which is the time required for the signal to increase from 10% to 90% of its amplitude, was also estimated.

2.6. GLAS geolocation accuracy

The GLA14 product includes the geolocation of each footprint, although it is subject to random errors. To evaluate the location accuracy of the footprints, their ground elevations were compared to the elevation values from the DEM derived from airborne LiDAR.

The DEM provided by the airborne LiDAR data vendor was resampled to 20 m. Given the low relief of the study area the spatial resampling was performed by considering the mean value of all pixels included within each 20 m pixel. Subsequently, elevations of the pixels lying within each footprint were weighted to take into account the Gaussian distribution of the energy within it (see Section 2.10 for more details). DEM values, which were employed as reference elevation, corresponded to orthometric elevations using the WGS-84 ellipsoid.

From GLAS data, the ground elevation is usually assumed to be the location of the last Gaussian peak fitted to the waveform. Nevertheless, Neuenschwander et al. (2008) found that in some cases a Gaussian function was fitted to receiver noise within the trailing edge of the waveform. To avoid this error and to ensure a true ground measurement for the last peak, the method proposed by Neuenschwander et al. (2008) was applied. Thus, an independent first derivative analysis was performed on the return waveform (GLA01); and those waveform peaks with amplitude higher than a signal threshold were matched to GLA14 first derivative modes. Since GLAS elevation corresponds to ellipsoidal elevation referenced to the TOPEX/Poseidon, the GLAS elevations were converted to the WGS-84 ellipsoid using the IDL Ellipsoid Conversion tool, downloaded from http://nsdic.org/data/icesat/tools.html. Because the horizontal shift between the two ellipsoids is negligible as compared to the accuracy of both datasets, only the vertical shift was considered. Subsequently, ellipsoidal elevations were converted to orthometric elevations by taking into account the geoid undulation.

Finally, the footprints were displaced within a 5×5 window, i.e. 100×100 m, centered on the nominal location provided by the GLA14 product. For each location, the correlation and the root mean square error (RMSE) were computed and that location that yielded the highest correlation and the lowest RMSE was considered as the correct location. A similar procedure was used by Popescu et al. (2011) and Sun et al. (2008).

2.7. Canopy cover

Canopy cover was computed for each footprint as the ratio of canopy energy to the total energy of the waveform. First, canopy energy was computed by summing the energy of the non-ground height bins; however, for the CC images derived from airborne data only those returns with a height greater than or equal to 2 m had been classified as belonging to the canopy. Therefore, to assess the effect of the different canopy definitions between airborne and satellite data, the canopy energy was also computed by only taking into account the energy of those height bins higher than or equal to 2 m. Moreover, the effect of applying different CBH thresholds, from 1 m to 4 m, was tested. Consequently, CC images were also created from airborne LiDAR height and intensity data at each CBH threshold. Also the canopy energy from GLAS waveforms was calculated for each CBH considered. Fig. 3 shows an example of canopy returns from airborne LiDAR and the canopy energy from GLAS data. The figure shows the difference in the proportion of energy that would be considered if canopy energy was computed from the upper limit of the ground energy (dashed line) to the signal beginning or if it was computed applying a CBH threshold (dash-dotted line).

2.8. Leaf area index

MacArthur and Horn (1969) proposed a method to estimate LAI which relates the percentage cover to the amount of foliage as a function of height, assuming a random horizontal distribution of foliage:

$$y_h = -\ln(1-\mathrm{cover}(h)) \quad (1)$$

where y_h is the cumulative LAI at height h and cover(h) is the fraction of sky obstructed by foliage above height h. This method was adapted by Lefsky et al. (1999) for use with large footprint full waveform data to derive the canopy height profile. Similarly, this method was applied to GLAS data and the results were evaluated for our study area. As in other studies (Harding et al., 2001; Lefsky et al., 1999; Means et al., 1999), a ratio of 2:1 was used to account for differences in ground and canopy reflectance at the wavelength of the GLAS laser. The CBH used to estimate LAI was 3.5 m as it was the height used to compute LAI from airborne data (Zhao & Popescu, 2009). It should be noted that since GLAS data considered both, the foliage and the woody material of the canopy, the plant area index (PAI) was actually estimated. PAI was also estimated from airborne LiDAR because no separation of wood versus foliage material was accomplished.

A second approach was attempted to estimate LAI by means of stepwise regression, which automatically selected the variables with the greatest explanatory power from the pool of metrics derived from GLAS data (Section 2.5). CC derived at 3.5 m was also used as the independent variable in the stepwise regression. For each footprint, the LAI values used to calibrate and validate the statistical model were extracted from airborne LiDAR-derived LAI image, as

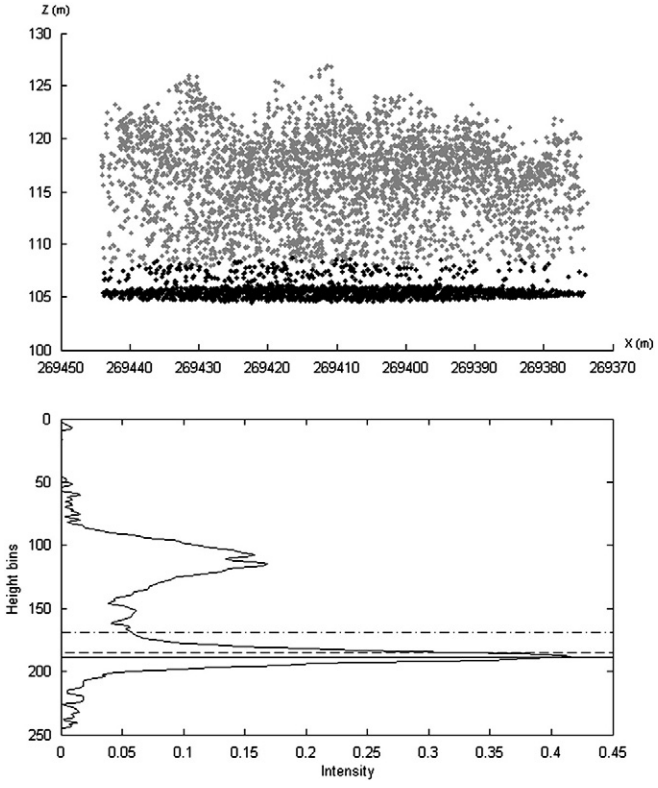

Fig. 3. Top: Airborne LiDAR data cloud point. Gray dots represent canopy returns (height ≥ 3 m). Black dots represent non canopy returns (height < 3 m). Bottom: Waveform and ground location (solid line), upper limit of the ground energy (dashed line) and canopy base height threshold (3 m) applied to compute canopy energy (dash-dotted line).

explained in Section 2.10. In order to provide a robust estimation of the parameters the jack-knife technique was applied, which systematically omits one observation at a time, and performs n-estimations of the parameters using $n-1$ observations. Finally the mean value of the n-estimations was selected as the definitive parameter, and a measure of dispersion, the standard deviation, was used to assess the uncertainty of parameter estimation. This method also provides information on the influence of each observation on the model. The Variance Inflation Factor (VIF) was also investigated to ensure that no collinearity was present in the selected model. In order to evaluate model performance a set of metrics proposed by Willmott (1982) was used in addition to the R^2 value, since the latter is often unrelated to the sizes of the difference between observed and predicted values. Table 1 describes the measures used to evaluate model performance.

2.9. Canopy bulk density

Several methods have been developed to estimate CBD from field measurements although their accuracy is unknown because it has never been measured directly in the field (Scott & Reinhardt, 2001). The methods proposed are based in several assumptions, such as the equal distribution of the fuel load throughout the crown, or that the shape of the crown fits a given geometrical figure. Hence, for uniform stands CBD can be calculated as the fuel load divided by canopy depth (Keane et al., 1998); however, the assumption of uniform stands is rarely fulfilled in most cases. To solve this limitation, Sando and Wick (1972) developed a methodology, subsequently modified by Beukema et al. (1997), which is used in numerous computer programs for the estimation of canopy fuel properties such as the Fire and Fuels Extension to the Forest Vegetation Simulator (FFE-FVS), FuelCalc or CrownMass. This approach first computes foliage and fine branch (<6 mm) biomass for every tree in the plot; the fuel load is then equally distributed into 1 foot (0.3048 m) bins through the crown of the tree. The fuel load contributed by each tree for every height bin is subsequently summed. The resulting vertical profile of the fuel load is smoothed by applying a running mean filter. Finally, CBD is estimated as the maximum of the smoothed canopy fuel profile.

This method was adapted to be applied to the data provided by GLAS based on the relationship between the energy recorded at each height bin and the amount of canopy material present at each height interval. A detailed description of how LiDAR waveforms and canopy structure are linked by the gap probability can be found in Ni-Meister et al. (2001). Thus, the LAI for each height interval, that is, the LAD (leaf area density, $m^2\ m^{-3}$) was computed. Subsequently the foliage biomass (FB) for each height interval was estimated by dividing the GLAS-derived LAI values ($m^2\ m^{-2}$) by the specific leaf area (SLA, $m^2\ kg^{-1}$) (Zhang & Kondragunta, 2006; Zhang et al., 2006). The SLA values used were those published by Pataki et al. (1998) for loblolly pine ($27.7\ cm^2\ g^{-1}$), which is the main species in the study area. Once derived the fuel vertical profile it was smoothed by applying a running mean. Two different values commonly used were tested, namely 3 m (Scott & Reinhardt, 2005; Scott & Reinhardt, 2007) and 4.5 m (Mitsopoulos & Dimitrakopoulos, 2007; Scott & Reinhardt, 2001). Finally, the CBD of the footprint was estimated as the maximum value of the smoothed canopy fuel profile. In addition, different CBH thresholds were applied when deriving the canopy fuel profile, from 2.5 m to 21.5 m at 0.5 m intervals, based on the minimum and

Table 1
Measures used for model performance evaluation.

Accuracy measurement	Definition	Characteristics
Root mean square error (RMSE)	$\sqrt{\frac{\sum_{i=1}^{N}(P_i-O_i)^2}{N}}$	O_i: Observed value. P_i: Model-predicted value. N. Number of observations.
Mean absolute difference (MAE)	$\frac{\sum_{i=1}^{N}\lvert P_i-O_i\rvert}{N}$	MAE and RMSE are similar measures; however MAE is less sensitive to extreme values.
Systematic root mean square error ($RMSE_S$)	$\sqrt{\frac{\sum_{i=1}^{N}(\hat{P}_i-O_i)^2}{N}}$	$\hat{P}_i$: Estimated value based on the ordinary least-squares regression, $\hat{P}_i = a + bO_i$. Explains how much of RMSE is systematic, and assess the model errors that are predictable. It should approach to zero.
Unsystematic root mean square error ($RMSE_U$)	$\sqrt{\frac{\sum_{i=1}^{N}(P_i-\hat{P}_i)^2}{N}}$	Explains how much of RMSE is unsystematic, and therefore is not predictable mathematically. It should approach to RMSE
Index of agreement (d)	$1-\left[\frac{\sum_{i=1}^{N}(P_i-O_i)^2}{\sum_{i=1}^{N}(\lvert P'_i\rvert+\lvert O'_i\rvert)^2}\right]_{0\le d\le 1}$	$P'_i = P_i-\bar{O}$ $O'_i = O_i-\bar{O}$ $\bar{O}$: is the mean observed value d: is a descriptive measure which can be widely applied to make cross-comparisons between models.

maximum values obtained by Zhao et al. (2011) using field data for this study area.

2.10. Validation of GLAS estimates

GLAS estimates of canopy fuel properties were validated using the products derived from airborne LiDAR data (Section 2.4). Thus, the values of the pixels included within each footprint were averaged to obtain the reference data with which GLAS estimates were compared. Moreover, given the Gaussian distribution of the energy within a footprint, the values of each pixel within it were weighted based on the distance to the center of the footprint using the following formula (Chen, 2010; Neuenschwander et al., 2008):

$$w = e^{\left(-2\sqrt{\left(\frac{x'}{a}\right)^2+\left(\frac{y'}{b}\right)^2}\right)}$$
$$x' = (x-x_0)\sin\alpha + (y-y_0)\cos\alpha \quad (2)$$
$$y' = (y-y_0)\sin\alpha - (x-x_0)\cos\alpha$$

where w is the weight of each pixel within a GLAS footprint, a and b are the semi-major and semi-minor axes of the footprint respectively, which are included in GLA14 product; (x,y) and (x_0,y_0) are the coordinates of the pixel and the footprint center respectively; x' and y' are the coordinates of the pixel along the major and minor axes, and α is the azimuth angle of the major-axis of the footprint, which is also included in the GLA14 product. The weights were normalized to sum to 1 before averaging.

3. Results

3.1. GLAS geolocation accuracy

The minimum R^2 found between the ALS-derived DEM and the GLAS ground elevation was 0.964 (row, column: 5, 5) and the maximum was 0.988 (row, column: 0, −1), whereas for the nominal location of the footprint, the R^2 obtained was 0.987. It can be seen that the range of R^2 values was only about 2%. The RMSE values found were 1.86 m, 1.49 m and 1.36 m, respectively. Nevertheless, despite the R^2 value was slightly higher for the location considered as correct (0, −1) as compared to the nominal location, its RMSE was also slightly higher; although differences between the two locations were insignificant in both cases.

3.2. Canopy cover

Canopy cover estimated as the ratio of canopy energy to the total energy of the waveform without applying any CBH threshold, showed a log trend (Fig. 4-left) with 57.6% of the variance explained.

Table 2
Coefficient of determination and RMSE values for the different CC estimates.

Canopy cover			
CBH	ALS	R^2	RMSE (%)
1 m	Range	0.54	18.34
	Intensity	0.60	15.62
2 m	Range	0.68	20.90
	Intensity	0.75	16.83
3 m	Range	0.79	20.93
	Intensity	0.87	16.63
4 m	Range	0.81	20.84
	Intensity	0.89	16.59

Results were improved when canopy energy was computed by applying a CBH threshold. Table 2 shows the R^2 and the RMSE values obtained for different CBHs applied and for the two reference datasets used, that is, CC derived from height and from intensity airborne LiDAR data.

It can be observed that results improved as the CBH threshold applied increased although the differences became negligible for CBH values of 3 and 4 m. More importantly when a CBH threshold was applied a linear relationship between GLAS and airborne LiDAR was obtained (Fig. 4-right). The table also shows that a better agreement was found between GLAS CC estimates and airborne LiDAR CC estimates when the latter was derived from intensity data.

3.3. Leaf area index

Table 3 shows the R^2, RMSE and the slope and offset values of the regression lines for the two methods used to estimate LAI from GLAS.

MacArthur and Horn's method yielded a good correlation with LAI estimations from airborne LiDAR although the RMSE was very high for the LAI values found in the study area (mean LAI = 1.5). The LAI values derived from this approach greatly underestimated LAI values as compared to values derived from airborne data. Estimation of LAI using stepwise regression yielded a very good agreement with airborne LiDAR, with an R^2 value of 0.9 and an RMSE of 0.15. The model included canopy cover and the leading edge extent as explanatory variables (Eq. 3). Both variables were statistically significant at the 99% with p-values <0.01.

$$LAI_{GLAS} = 0.416 + 0.025^{*}CC + 0.012^{*}LE \quad (3)$$

The model presented no collinearity according to the VIF values obtained (1.5 and 1.8 for CC and LE, respectively). Although there is no unanimity regarding what values of VIF indicate the existence of collinearity between the explanatory variables, it is commonly accepted that values above 10 are indicative of collinearity. As for the analysis of residuals, no trend or heteroscedasticity was observed. The standard

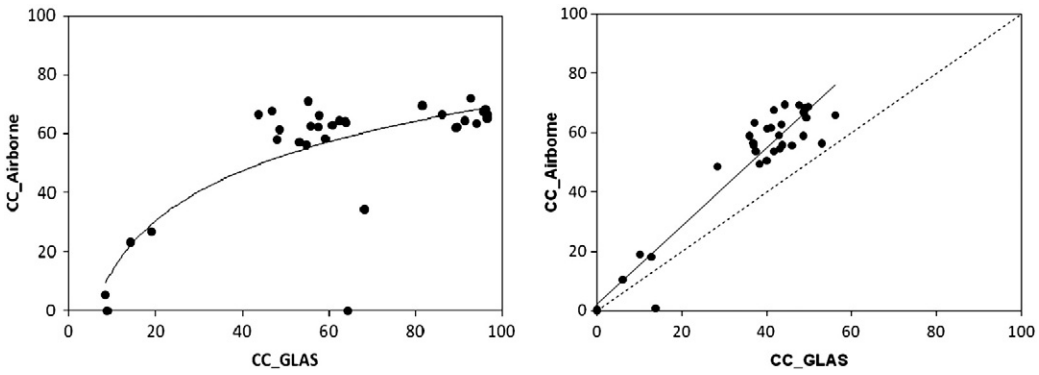

Fig. 4. Left) CC estimated from GLAS data without applying any CBH threshold versus CC estimated from airborne LiDAR data (CBH = 2 m). Right) CC estimated from GLAS data applying a 3 m CBH threshold versus CC estimated from airborne LiDAR intensity data applying a 3 m CBH threshold (dashed line represents the Y = X line).

Table 3
Comparison of the methods used to estimate LAI from GLAS data.

Leaf area index				
Method	R^2	RMSE	Slope	Offset
MacArthur's and Horn's	0.73	1.00	1.36	0.76
Stepwise regression	0.9	0.15	1.0008	0.0005

deviations of the estimated parameters were very low, 0.0124, 0.0004 and 0.0005 for the independent term, CC and LE, respectively. This low standard deviation indicates an accurate estimation of parameters and that no single observation had a large influence. The model showed good performance as indicated by the R^2 and index of agreement (d) values, 0.9 and 0.97 respectively. In addition, the systematic component of the RMSE was close to zero ($RMSE_S = 0.05$) whereas the unsystematic component ($RMSE_U = 0.14$) was close to the RMSE as it is expected for a good model. Fig. 5 shows GLAS estimates by the empirical approach versus airborne estimates.

3.4. Canopy bulk density

The method proposed to compute CBD yielded the best result when applying a CBH threshold of 11.5 m to derive the canopy fuel profile, which was the mean field measured CBH of the study area (Zhao et al., 2011), with an R^2 of 0.78 and an RMSE of 0.02 kg m^{-3}. These values were obtained using a running mean of 3 m, which generally provided slightly more accurate results than a 4.5 m running mean, due to its lower generalization of the profile. The R^2 values obtained for different CBH thresholds varied between 0.01 and 0.78. The lowest R^2 value corresponded to a CBH of 21.5 m as consequence of a large number of footprints with a vegetation height lower than that threshold. The method generally underestimated CBD as compared to airborne derived CBD. Fig. 6 shows GLAS versus airborne estimated CBD. The slope of the trend line was not significantly different from 1 (1.118; p-value > 0.05) nevertheless the aspect was significantly different from 0 (0.0182; p-value < 0.05) indicating a bias in the estimates.

4. Discussion

4.1. GLAS geolocation accuracy

The correct location was found by shifting the footprints one column so that the error of the GLAS footprints was less than 20 m. These results agree with the errors found by Popescu et al. (2011), who reported an estimated error of 25.5 ± 11.6 m for the same study area. Similar geolocation errors were obtained by Sun et al. (2008) when comparing GLAS data to SRTM DEM data over a forested area in Maryland, USA.

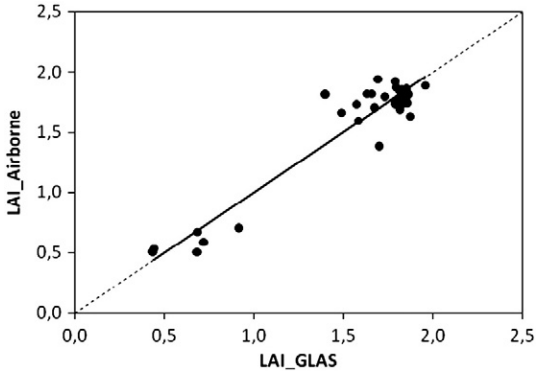

Fig. 5. GLAS versus airborne LAI estimates (dashed line represents the Y = X line).

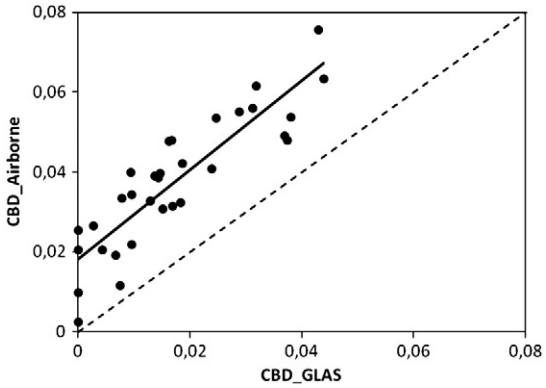

Fig. 6. GLAS versus airborne CBD estimates (dashed line represents the Y = X line).

The errors found in the determination of ground elevations were approximately 1.5 m; these are higher than the errors achieved by Popescu et al. (2011) after manually identifying the ground peak, but smaller than the errors obtained by using the same automatic procedure used in this study. The differences found despite using the same study area and the same automatic ground-finding procedure might be explained because they evaluated the ground elevation using a multitemporal GLAS dataset captured using different lasers, which increased the variability of the data. Furthermore, changes in the vegetation cover between GLAS campaigns contributed to problems in identifying the ground peak, explaining the higher differences found by them.

4.2. Canopy cover

Canopy cover estimated from GLAS data without any CBH threshold yielded a log trend when compared to the airborne LiDAR. Neuenschwander et al. (2008) also found a log trend between full waveform airborne LiDAR and GLAS data in San Marcos, Texas, although the R^2 value was higher (0.736). The log relationship found when no CBH threshold was applied may be explained by the fact that in such a case, the canopy energy considered within each GLAS footprint includes understory vegetation that was not included for airborne LiDAR. Thus, when the same CBH was applied to both datasets, the R^2 values increased significantly, and the relationship became linear. Moreover, the correlation between the two datasets increased with the increase in CBH. Popescu et al. (2011) found that the height of lower percentiles of the energy of the GLAS footprints had a weak correlation with the lower percentiles derived from airborne LiDAR data, which may be a consequence of the scan angle of the airborne data and the pulse width of the GLAS. Holmgren et al. (2003) found that scanning angle had a large impact of canopy closure estimates. The weaker correlation between the two datasets for lower percentiles is also reflected by the worse results obtained for lower CBH values.

The use of intensity data to generate CC from airborne LiDAR showed better agreement (around 7%) with GLAS data than the use of the range. This can be explained because the GLAS sensor digitizes the amount of energy reflected off the target, and so it records the intensity of the laser return. When the range capability of airborne LiDAR data is used, only the presence/absence of a reflection surface is accounted for but not the amount of energy returned to the sensor.

4.3. Leaf area index

Both methods used to estimate LAI from GLAS showed good correlation with airborne estimates although MacArthur and Horn's method showed a very large underestimation of LAI values. This method has been shown to underestimate total LAI when foliage is clumped

and foliage density is high (Aber, 1979; Hosoi & Omasa, 2006). Airborne LiDAR estimates were not corrected for clumping and so, the underestimation of LAI values when compared to the reference data could be explained as a consequence of the scan angle, because the airborne LiDAR sampled the canopy from different angles whereas GLAS observations were at nadir.

The ratio applied to take into account the different reflectance of ground and canopy at the 1064 nm was 2:1; nevertheless, this ratio is site dependent so a better adjusted ratio for this study area, based for example on field spectroradiometric measurements, could improve the results.

As for the regression model obtained, this showed a very good agreement with airborne-derived LAI values. The RMSE value obtained represents the 7.7% of the mean airborne derived LAI values for the study area. Canopy cover and leading edge were selected as explanatory variables in the model. The latter variable is related not only to canopy height variability (Lefsky et al., 2007) but also to the density of the canopy, with lower values for more dense canopies. Lefsky et al. (1999) estimated LAI from SLICER data and found that the most important variable for predicting LAI was the filled canopy volume, which was described as a three-dimensional analog of the cover. Filled canopy volume has the advantage over canopy cover in that it is sensitive to LAI increases after canopy closure, whereas an asymptotic relationship can be found between canopy cover and LAI values larger than 3. Since LAI values for the area used in this study were smaller than 3 no asymptotic relationship was observed.

4.4. Canopy bulk density

The results obtained for CBD showed good agreement between GLAS and airborne estimates although CBD was underestimated and the RMSE represented nearly 40% of the mean CBD of the study area. Nevertheless, since the slope of the trend line between GLAS and airborne estimates was not statistically different from 1, the systematic underestimation of GLAS-derived CBD could be compensated by adding the bias term.

The errors of the CBD estimates can be partly explained by different factors. The first reason is the different definition of CBD used by Zhao et al. (2011) and the one used in this study. Thus they estimated CBD considering as available fuel both, foliage and fine branches (<6 mm); whereas in this study only the foliage biomass was considered. Second, the estimation of the fuel profile is based on MacArthur and Horn's method, which underestimates the LAI used to derive FB. Nevertheless, since GLAS waveform measures all vegetative components, foliage and woody biomass, PAI is actually estimated not LAI so this effect would be partially compensated. In addition, the SLA values used to transform LAI to FB were obtained from a different area. Moreover, a unique SLA value was used, whereas the study area presented several species. Also the large footprint of ICESat might not provide as much detail of the canopy structure as the airborne LiDAR.

The use of different CBH values, which ranged between 2.75 m and 21.04 m (Zhao et al., 2011), to derive the canopy fuel profile greatly affected the results due to its high variability. If methods were derived to automatically identify canopy bins, a different CBH threshold could be applied to each footprint, which would improve the results.

Another factor to be considered is the error associated to the reference data used to validate GLAS estimates. The RMSE reported by Zhao et al. (2011) for the CBD estimated using ALS data was 0.015 kg m^{-3}, which is almost as high as the error obtained for GLAS data.

5. Conclusions

This research has shown the potential of the ICESat/GLAS sensor to estimate canopy fuel properties relevant for crown fire behavior as compared to data derived from airborne LiDAR data collected over the same area. An analysis of the geolocation accuracy of GLAS data showed an offset less than one pixel (20 m). Canopy cover has been successfully estimated as the ratio of the canopy energy to the total energy of the waveform. It has been shown that the relationship between airborne and satellite estimates of CC became linear when a CBH threshold was applied since no understory vegetation was included to compute canopy energy. Moreover, the amount of variance explained increased as the CBH threshold applied increased. Also, better correlation was found when CC was derived from the intensity of the airborne LiDAR data.

LAI was estimated from two different approaches. MacArthur and Horn's method greatly underestimated LAI, which agrees with other studies using discrete return LiDAR. Better estimates were obtained using an empirical model derived using a stepwise regression approach. However, empirical models are limited in terms of generalization capability since extrapolation of the equations to areas different to that used for calibration can yield unreliable results.

Canopy bulk density was estimated based on the approached developed by Sando and Wick (1972), commonly used in computer tools used for forest fuel management such as FFE-FVS or the CrownMass to estimate CBD from field data. The method was adapted to the GLAS data and showed good agreement with CBD estimates from airborne LiDAR. This method has more generalization capability than empirical methods and could be applied to different areas if FB or SLA values can be derived from other sources such as MODIS products (Heinsch et al., 2003; Zhang & Kondragunta, 2006).

Future satellite LiDAR missions with smaller footprints might provide a better description of the structure of the canopy providing closer estimates to airborne LiDAR estimates.

The study area represents a gentle topography which reduced the impact of slope and terrain roughness on the derivation of parameters from GLAS data. Future studies should evaluate the potential of GLAS to estimate the canopy fuel properties over more complex terrain to test the generalization power at regional and global scales of the methods presented.

Acknowledgements

This research was carried out during a visit of the first author to the Spatial Sciences Laboratory, Department of Ecosystem Science and Management, Texas A&M University, funded by the University of Alcalá. Comments made by the anonymous reviewer are greatly appreciated.

References

Aber, J. D. (1979). Foliage-height profiles and succession in Northern Hardwood forests. *Ecology*, *60*, 18–23.

Albini, F. A., & Baughman, R. G. (1979). Estimating windspeeds for predicting wildland fire behavior. *Research Paper INT-221, USDA, Forest Service, Intermountain Forest and Range Experiment Station, Odgen, Utah*.

Andersen, H. -E., McGaughey, R. J., & Reutebuch, S. E. (2005). Estimating forest canopy fuel parameters using LIDAR data. *Remote Sensing of Environment*, *94*, 441–449.

Ashworth, A., Evans, D. L., Cooke, W. H., Londo, A., Collins, C., & Neuenschwander, A. L. (2010). Predicting southeastern forest canopy heights and fire fuel models using GLAS data. *Photogrammetric Engineering & Remote Sensing*, *76*, 915–922.

Beukema, S. J., Greenough, D. C., Robinson, C. E., Kurtz, W. A., Reinhardt, E. D., Crookston, N. L., et al. (1997). An introduction to the fire and fuels extension to FVS. In R. Teck, M. Mouer, & J. Adams (Eds.), *Proceedings of the Forest Vegetation Simulator conference;1997 February 3–7; Fort Collins, CO. Gen. Tech. Rep. INT-373* (pp. 191–195). Ogden, UT: U.S. Department of Agriculture, Forest Service, Intermountain Research Station.

Boudreau, J., Nelson, R. F., Margolis, H. A., Beaudoin, A., Guindon, L., & Kimes, D. S. (2008). Regional aboveground forest biomass using airborne and spaceborne LiDAR in Québec. *Remote Sensing of Environment*, *112*, 3876–3890.

Brenner, A. C., Zwally, H. J., Bentley, C. R., Csatho, B. M., Harding, D. J., Hofton, M. A., et al. (2003). Geoscience laser altimeter system algorithm theoretical basis document: Derivation of range and range distributions from laser pulse waveform analysis. *Algorithm Theoretical Basis Documents (ATBD)*http://www.csr.utexas.edu/glas/atbd.html [Online]. Available

Carabajal, C. C., & Harding, D. J. (2006). SRTM C-Band and ICESat laser altimetry elevation comparisons as a function of tree cover and relief. *Photogrammetric Engineering & Remote Sensing*, *72*, 287–298.
Chen, Q. (2010). Retrieving vegetation height of forests and woodlands over mountainous areas in the Pacific Coast region using satellite laser altimetry. *Remote Sensing of Environment*, doi:10.1016/j.rse.2010.1002.1016.
Chuvieco, E., Riaño, D., van Wagtendonk, J., & Morsdorf, F. (2003). Fuel loads and fuel types. In E. Chuvieco (Ed.), *Wildland fire danger estimation and mapping. The role of remote sensing data* (pp. 1–32). Singapore: World Scientific Publishing Co. Ltd.
Donoghue, D. N. M., Watt, P. J., Cox, N. J., & Wilson, J. (2007). Remote sensing of species mixtures in conifer plantations using LiDAR height and intensity data. *Remote Sensing of Environment*, *110*, 509–522.
Drake, J. B., Dubayah, R. O., Knox, R. G., Clark, D. B., & Blair, J. B. (2002). Sensitivity of large-footprint LiDAR to canopy structure and biomass in a neotropical rainforest. *Remote Sensing of Environment*, *81*, 378–392.
Duong, H., Lindenbergh, R., Pfeifer, N., & Vosselman, G. (2009). ICESat full-waveform altimetry compared to airborne laser altimetry over The Netherlands. *IEEE Transactions on Geoscience and Remote Sensing*, *47*, 3365–3378, doi:10.1109/TGRS.2009.2021468.
Erdody, T. L., & Moskal, L. M. (2009). *Fusion of LiDAR and imagery for estimating forest canopy fuels.* : Remote Sensing of Environment.
García, M., Riaño, D., Chuvieco, E., & Danson, F. M. (2010). Estimating biomass carbon stocks for a Mediterranean forest in Spain using height and intensity LiDAR data. *Remote Sensing of Environment*, *114*, 816–830.
Hall, S. A., Burke, I. C., Box, D. O., Kaufmann, M. R., & Stoker, J. M. (2005). Estimating stand structure using discrete-return LiDAR: An example from low density, fire prone ponderosa pine forests. *Forest Ecology and Management*, *208*, 189–209.
Harding, D., & Carabajal, C. C. (2005). ICESat waveform measurements of within-footprint topographic relief and vegetation vertical structure. *Geophysical Research Letters*, *32*, doi:10.1029/2005GL023471.
Harding, D. J., Lefsky, M. A., Parker, G. G., & Blair, J. B. (2001). Laser altimeter canopy height profiles: Methods and validation for closed-canopy, broadleaf forests. *Remote Sensing of Environment*, *76*, 283–297.
Heinsch, F. A., Reeves, M., Votava, P., Kang, S., Milesi, C., Zhao, M., et al. (2003). User's Guide GPP and NPP (MOD17A2/A3) products NASA MODIS land algorithm. *Sch. of For., Univ. of Mont., Missoula, Mont*http://www.ntsg.umt.edu/modis/MOD17UsersGuide.pdf (Available at
Hofton, M. A., Minster, J. B., & Blair, J. B. (2000). Decomposition of laser altimeter waveforms. *IEEE Transactions on Geoscience and Remote Sensing*, *38*, 1989–1996.
Holmgren, J., Nilsson, M., & Olsson, H. (2003). Simulating the effects of LiDAR scanning angle for estimation of mean tree height and canopy closure. *Canadian Journal of Remote Sensing*, *29*, 623–632.
Hosoi, F., & Omasa, K. (2006). Voxel-based 3-D modeling of individual trees for estimating leaf area density using high-resolution portable scanning LiDAR. *IEEE Transactions on Geoscience and Remote Sensing*, *44*, 3610–3618.
Keane, R. E., Garner, J. L., Schmidt, K. M., Long, D. G., Menakis, J. P., & Finney, M. A. (1998). Development of input data layers for the FARSITE fire growth model for the Selway-Bitterroot Wilderness complex, USA. *Gen. Tech. Rep. RMRS-GTR-3*. Ogden, UT: U.S. Department of Agriculture, Forest Service, Rocky Mountain Research Station.
Keane, R. E., Reinhardt, E. D., Scott, J., Gray, K., & Reardon, J. (2005). Estimating forest canopy bulk density using six indirect methods. *Canadian Journal of Forest Research*, *35*, 724–739.
Lefsky, M. A., Cohen, W. B., Acker, S. A., Parker, G. G., Spies, T. A., & Harding, D. (1999). LiDAR remote sensing of the canopy structure and biophysical properties of Douglas-fir Western Hemlock forests. *Remote Sensing of Environment*, *70*, 339–361.
Lefsky, M. A., Harding, D. J., Keller, M., Cohen, W. B., Carabajal, C. C., del Bom Espirito-Santo, F., et al. (2006). Estimates of forest canopy height and aboveground biomass using ICESat. *Geophysical Research Letters*, *33*, doi:10.1029/2005GL025518.
Lefsky, M. A., Keller, M., Pang, Y., de Camargo, P. B., & Hunter, M. O. (2007). Revised method for forest canopy height estimation from Geoscience Laser Altimeter System waveforms. *Journal of Applied Remote Sensing*, *1*, doi:10.1117/1111.2795724.
Lefsky, M. (2010). A global forest canopy height map from the Moderate Resolution Imaging Spectroradiometer and the Geoscience Laser Altimeter System. *Geophysical Research Letters*, *37*, L15401, doi:10.1029/2010GL043622.
MacArthur, R. H., & Horn, H. S. (1969). Foliage profile by management vertical measurements. *Ecology*, *50*, 802–804.
Means, J. E., Acker, S. A., Harding, D. J., Blair, J. B., Lefsky, M. A., Cohen, W. B., et al. (1999). Use of large-footprint scanning airborne LiDAR to estimate forest stand characteristics in the western Cascades of Oregon. *Remote Sensing of Environment*, *67*, 298–308.
Mitsopoulos, I. D., & Dimitrakopoulos, A. P. (2007). Canopy fuel characteristics and potential crown fire behavior in Aleppo pine (*Pinus halepensis* Mill.) forests. *Annals of Forest Science*, *64*, 287–299.
Morsdorf, F., Kotz, B., Meier, E., Itten, K. I., & Allgöwer, B. (2006). Estimation of LAI and fractional cover from small footprint airborne laser scanning data based on gap fraction. *Remote Sensing of Environment*, *104*, 50–61.
Morsdorf, F., Meier, E., Kotz, B., Itten, K. I., Dobbertin, M., & Allgower, B. (2004). LiDAR-based geometric reconstruction of boreal type forest stands at single tree level for forest and wildland fire management. *Remote Sensing of Environment*, *92*, 353–362.
Nelson, R. (2010). Model effects on GLAS-based regional estimates of forest biomass and carbon. *International Journal of Remote Sensing*, *31*, 1359–1372.
Neuenschwander, A. L., Magruder, L. A., & Tyler, M. (2009). Landcover classification of small-footprint, full-waveform LiDAR data. *Journal of Applied Remote Sensing*, *3*, doi:10.1117/1111.3229944.
Neuenschwander, A. L., Urban, T. J., Gutierrez, R., & Schutz, B. E. (2008). Characterization of ICESat/GLAS waveforms over terrestrial ecosystems: Implications for vegetation mapping. *Journal of Geophysical Research*, *113*, doi:10.1029/2007JG000557.
Ni-Meister, W., Jupp, D. L. B., & Dubayah, R. (2001). Modeling lidar waveforms in heterogeneous and discrete canopies. *IEEE Transactions on Geoscience and Remote Sensing*, *39*, 1943–1958.
Pataki, D. E., Oren, R., & Phillips, N. (1998). Responses of sap flux and stomatal conductance of *Pinus taeda* L. trees to stepwise reductions in leaf area. *Journal of Experimental Botany*, *49*(322), 871–878.
Peterson, B.E. (2005). Canopy fuels inventory and mapping using large-footprint LiDAR. PhD. Dissertation. Faculty of the Graduate School of the University of Maryland, College Park
Popescu, S., & Zhao, K. (2008). A voxel-based LiDAR method for estimating crown base height for deciduous and pine trees. *Remote Sensing of Environment*, *112*, 767–781.
Popescu, S. C., Zhao, K., Neuenschwander, A., & Lin, C. (2011). Satellite lidar vs. small footprint airborne lidar: Comparing the accuracy of aboveground biomass estimates and forest structure metrics at footprint level. *Remote Sensing of Environment*, *115*, 2786–2797.
Reeves, M. C., Ryan, K. C., Rollins, M. G., & Thompson, T. G. (2009). Spatial fuel data products of the LANDFIRE Project. *International Journal of Wildland Fire*, *18*, 250–267.
Riaño, D., Chuvieco, E., Condes, S., Gonzalez-Matesanz, J., & Ustin, S. L. (2004). Generation of crown bulk density for *Pinus sylvestris* L. from LiDAR. *Remote Sensing of Environment*, *92*, 345–352.
Riaño, D., Meier, E., Allgower, B., Chuvieco, E., & Ustin, S. L. (2003). Modeling airborne laser scanning data for the spatial generation of critical forest parameters in fire behavior modeling. *Remote Sensing of Environment*, *86*, 177–186.
Riaño, D., Valladares, F., Condes, S., & Chuvieco, E. (2004). Estimation of leaf area index and covered ground from airborne laser scanner (LiDAR) in two contrasting forests. *Agricultural and Forest Meteorology*, *124*, 269–275.
Rothermel, R. C., Wilson, R. A., Morris, G. A., & Sackett, S. S. (1986). Modeling moisture content of fine dead wildland fuels input to the BEHAVE fire prediction system. *Research Paper INT-359, USDA, Forest Service, Odgen, Utah*.
Sandberg, D. V., Ottmar, R. D., & Cushon, G. H. (2001). Characterizing fuels in the 21st Century. *International Journal of Wildland Fire*, *18*, 381–387.
Sando, R. W., & Wick, C. H. (1972). A method of evaluating crown fuels in forest stands. *Res. Pap. NC-4*. Saint Paul, MN: U.S. Department of Agriculture, Forest Service, North Central Forest Experiment Station.
Scott, J., & Reinhardt, E. D. (2001). Assessing crown fire potential by linking models of surface and crown fire behavior. *Research Paper RMRS-RP-29, USDA Forest Service, Rocky Mountain Research Station*.
Scott, J., & Reinhardt, E. D. (2005). Stereo photo guide for estimating canopy fuel characteristics in conifer stands. *General technical report RMRS-GTR-145, USDA Forest Service, Rocky Mountain Research Station*.
Scott, J., & Reinhardt, E. D. (2007). Effects of alternative treatments on canopy fuel characteristics in five conifer stands. *General Technical Report PSW-GTR-203, USDA Forest Service, Rocky Mountain Research Station*.
Schutz, B. E., Zwally, H. J., Shuman, C. A., Hancock, D., & DiMarzio, J. P. (2005). Iveriview of the ICESat Mission. *Geophysical Research Letters*, *32*, doi:10.1029/2005GL024009.
Solberg, S., Brunner, A., Hanssen, K. H., Lange, H., Næsset, E., Rautiainen, M., et al. (2009). Mapping LAI in a Norway spruce forest using airborne laser scanning. *Remote Sensing of Environment*, *113*, 2317–2327.
Starek, M., Luzum, B., Kumar, R., & Slatton, K. C. (2006). Normalizing Lidar intensities. *Geosensing Engineering and Mapping (GEM)*. University of Florida: Civil and Coastal Engineering Department.
Sun, G., Ranson, K. J., Kimes, D. S., Blair, J. B., & Kovacs, K. (2008). Forest vertical structure from GLAS: An evaluation using LVIS and SRTM data. *Remote Sensing of Environment*, *112*, 107–117.
Van Wagner, C. E. (1977). Conditions for the start and spread of crown fire. *Canadian Journal of Forest Research*, *7*, 23–34.
Willmott, C. J. (1982). Some comments on the evaluation of model performance. *Bulletin of American Meteorological Society*, *63*, 1309–1313.
Xing, Y., de Gier, A., Zhang, J., & Wang, L. (2010). An improved method for estimating forest canopy height using ICESat-GLAS full waveform data over sloping terrain: A case study un Changbai mountains, China. *International Journal of Applied Earth Observation and Geoinformation*, doi:10.1016/j.jag.2010.1004.1010.
Zhang, X., & Kondragunta, S. (2006). Estimating forest biomass in the USA using generalized allometric models and MODIS land products. *Geophysical Research Letters*, *33*, doi:10.1029/2006GL025879.
Zhang, X., Kondragunta, S., Kogan, F., Guo, W., & Schmidt, C. (2006). Satellite-derived pm2.5 emissions from wildfires for air quality forecast. *15th Annual Emission Inventory Conference, May 16–18, 2006, in New Orleans*.
Zhao, K., & Popescu, S. (2009). LiDAR-based mapping of leaf area index and its use for validating GLOBCARBON satellite LAI product in a temperate forest of the southern USA. *Remote Sensing of Environment*, *113*, 1628–1645.
Zhao, K., Popescu, S., Meng, X., Pang, Y., & Agca, M. (2011). Characterizing forest canopy structure with LiDAR composite metrics and machine learning. *Remote Sensing of Environment*, doi:10.1016/j.rse.2011.04.001.
Zwally, H. J., Schutz, B., Abdalati, W., Abshire, J., Bentley, C., Brenner, A., et al. (2002). ICESat's laser measurements of polar ice, atmosphere, ocean, and land. *Journal of Geodynamics*, *34*, 405–445.